

1 Article

2 Critical role of an MHC Class I-like/innate-like T cell 3 immune surveillance system in host defense against 4 ranavirus (Frog virus 3) infection.

5 Edholm, Eva-Stina*^{1,2}, Francisco De Jesús Andino*¹, Jinyeong Yim¹, Katherine Woo¹, and Jacques
6 Robert¹

7 ¹ Department of Microbiology and Immunology, University of Rochester Medical Center, Rochester,
8 NY, USA.

9 ² The Norwegian College of Fishery Science, University of Tromsø, the Arctic university of Norway,
10 Tromsø, Norway.

11 * These authors contributed equally to this work.

12 Communicating Author: Dr. Jacques Robert, Department of Microbiology and Immunology, University of
13 Rochester Medical Center, Rochester, NY 14642; Phone (585) 275-1722; FAX (585) 473-9573; e-mail:

14 Jacques_Robert@urmc.rochester.edu
15

16 **Abstract:** Besides the central role of classical MHC class Ia-restricted conventional CD8 T cells in
17 antiviral host immune response, the amphibian *Xenopus laevis* critically rely on MHC class I-like
18 (*mhc1b10.1.L* or XNC10)-restricted innate-like (iT) cells (iV α 6 T cells) to control infection by the
19 ranavirus Frog virus 3 (FV3). To complement and extend our previous reverse genetic studies
20 showing that iV α 6 T cells are required for tadpole survival as well as for timely and effective adult
21 viral clearance, we examined the conditions and kinetics of iV α 6 T cell response against FV3. Using
22 a FV3 knock-out (KO) growth-defective mutant, we found that upregulation of the XNC10
23 restricting class I-like gene and the rapid recruitment of iV α 6 T cells depend on detectable viral
24 replication and productive FV3 infection. In addition, by *in vivo* depletion with XNC10 tetramers
25 we demonstrated the direct antiviral effector function of iV α 6 T cells. Notably, the transitory iV α 6
26 T cell defect delayed innate interferon and cytokines gene response resulting in long-lasting
27 negative inability to control FV3 infection. These findings suggest that in *Xenopus* and likely other
28 amphibians, an immune surveillance system based on the early activation of iT cells by non-
29 polymorphic MHC class-I like molecules is important for efficient antiviral immune response.
30

31 **Keywords:** Unconventional T cell; nonclassical MHC; antiviral immunity; interferon
32

33 1. Introduction

34 In mammals, potent adaptive immune response against viral pathogens largely depend on
35 conventional CD8 T cell effectors that express a broad T cell receptor (TCR) repertoire capable of
36 recognizing a large array of antigens presented by polymorphic classical MHC class I molecules (class
37 Ia). However, it is increasingly appreciated that other unconventional or innate-like T cell effectors
38 are critically involved in antiviral immunity (Reviewed in (Adams and Luoma, 2013)). These iT cells
39 interact with non-polymorphic MHC class I-like molecules, have a limited or invariant TCR
40 repertoire and are thought to serve as important early responders and immune regulators. One of the
41 best characterized iT cell population are iNKT cells that are restricted by the MHC class I-like
42 molecule CD1d that present lipids (Borg et al., 2007; Rossjohn et al., 2012). The antiviral role of iNKT
43 cells has been shown for murine cytomegalovirus (MCMV; (Wesley et al., 2008), lymphocytic

44 choriomeningitis virus (LCMV; (Diana et al., 2009)), herpes simplex virus 1 (HSV1;(Raftery et al.,
45 2008)), HIV and influenza (Juno et al., 2012) and even for vaccinia virus (VAC; (Abboud et al., 2016).

46 In the amphibian *Xenopus laevis*, while adult frogs exhibit an immune system whose
47 conventional class Ia-restricted CD8 T cell compartment is dominant as in mammals, tadpoles are
48 immunocompetent but are naturally class Ia-deficient and primarily rely on MHC class I-like and iT
49 cells to mediate immunity (Edholm et al., 2016). Deep-sequencing repertoire analysis has revealed
50 the over-representation of 6 invariant TCR α rearrangements implying the predominance of 6 larval
51 iT cell subsets (Edholm et al., 2013). One of the 6 putative iT cell subsets, the iV6 T cell subset,
52 expresses the rearranged V α 6-J1.43 TCR α chain and requires the MHC class I-like molecule XNC10
53 (encoded by *mhc1b10.1.L*) for its thymic development and function (Edholm et al., 2013). Notably,
54 host immune responses against the ranavirus pathogen FV3 is significantly impaired by lack of iV α 6
55 T cells resulting from XNC10 loss-of-function. FV3 is a major pathogen of amphibians, fish and even
56 reptiles (Price et al., 2014). The dramatic worldwide increases in host ranges (i.e., populations and
57 species infected) and amphibian die-offs caused by RVs (see eBook (Gray and Chinchar, 2015)), raise
58 alarming concerns for biodiversity and aquaculture, and pose fundamental issues related to
59 evolution of host/pathogen interactions. As such, the involvement of iT cells in addition to
60 conventional CD8 T cells in antiviral host resistance is of high relevance.

61 In adult *X. laevis*, XNC10 deficiency considerably delays viral clearance resulting in increased
62 tissue damage (Edholm et al., 2015). As expected from iT cell prevalence in tadpoles, XNC10
63 deficiency markedly increases the mortality rate, especially at early stage of FV3 infection (Edholm
64 et al., 2013). The generation of XNC10 tetramers by expressing XNC10 fused to *X. laevis* beta 2 (b2m)-
65 microglobulin has permitted a better characterization of the iV α 6 T cell response kinetics and show
66 a rapid recruitment (within less than 24 hrs.) at the site of infection. This fast targeted response
67 suggests a sensitive detection mechanism of FV3 infection. However, many facets of this response
68 remain to be investigated including whether iV α 6 T cells require stimulation by XNC10 bound to
69 viral or other ligands, or can be activated by XNC10-independent co-stimulation signals (e.g., danger
70 signals, IFN response). To explore some of these issues we have taken advantage of our XNC10
71 tetramer as well as a FV3 recombinant virus deficient for a putative immune evasion gene to
72 determine the role of productive versus ablated viral infection as well as the effect of transiently
73 impairing iV α 6 T cell function at early stage of FV3 infection.

74 2. Material and methods:

75 2.1. Animals

76 All outbred *X. laevis* were from the *X. laevis* research resource for immunology at the University
77 of Rochester (<https://www.urmc.rochester.edu/microbiology-immunology/xenopus-laevis.aspx>). All
78 animals were handled in accordance with stringent laboratory and University Committee on Animal
79 Research regulations minimizing suffering (Approval number 100577/2003-151). For all experiments,
80 three-weeks old, tadpoles (stage 55, 1.5 cm long; ([Nieuwkoop and Faber, 1967](#))) and 1 year-old young
81 adult frogs were used.

82 2.2. Frog virus 3 stocks and infection

83 Baby hamster kidney cells (BHK-21, ATCC No. CCL-10) were maintained in DMEM (Invitrogen)
84 containing 10% fetal bovine serum (Invitrogen), streptomycin (100 μ g/mL), and penicillin (100 U/mL)
85 with 5% CO₂ at 37°C, then 30°C for infection. The generation and characterization of the FV3 knock-
86 out (KO) mutant Δ vCARD (or Δ 64R) has been detailed elsewhere (Andino Fde et al., 2015; Chen et
87 al., 2011; Jacques et al., 2017). Wild type (WT) and KO FV3 were grown using a single passage through
88 BHK-21 cells and were subsequently purified by ultracentrifugation on a 30% sucrose cushion. Adult
89 frogs were infected by i.p. injection of 1 \times 10⁶ PFU in 100 μ L of amphibian PBS (APBS) and tadpoles
90 were infected by i.p. injection of 10, 000 PFU in 5 μ L APBS. Uninfected control animals were mock-
91 infected with an equivalent volume of APBS. At different days post-infection (dpi), animals were

92 euthanized using 1 µg/L tricaine methanesulfonate (TMS) buffered with bicarbonate prior to
93 dissection and extraction of nucleic acids from tissues.

94 2.3. Quantitative gene expression analyses

95 Total RNA was extracted from peritoneal leucocytes and kidneys using Trizol reagent, following
96 the manufacturer's protocol (Invitrogen). cDNA was synthesized with 0.5 µg of RNA in 20 µl using
97 the iScript cDNA synthesis kit (Bio-Rad, Hercules, CA), and 1 µl of cDNA template was used in all
98 RT-PCRs and 150 ng DNA for PCR. Minus RT controls were included for every primer pair. A
99 water-only control was included in each reaction. The qPCR analysis was performed using the ABI
100 7300 real-time PCR system with PerfeCT SYBR Green FastMix, ROX (Quanta) and ABI sequence
101 detection system (SDS) software. Glyceraldehyde-3-phosphate dehydrogenase (GAPDH) controls
102 were used in conjunction with the $\Delta\Delta$ CT method to analyze cDNA for gene expression. All primer
103 sequences are listed in Table S1.

104 2.4. Viral load quantification by qPCR and plaque assay

105 FV3 viral loads were assessed by absolute qPCR by analysis of isolated DNA in comparison to
106 a serially diluted standard curve. Briefly, an FV3 DNA Pol II PCR fragment was cloned into the
107 pGEM-T Easy vector (Promega). This construct was amplified in bacteria, quantified and serially
108 diluted to yield 10^{10} - 10^1 plasmid copies of the vDNA POL II. These dilutions were employed as a
109 standard curve in subsequent absolute qPCR experiments to derive the viral genome transcript copy
110 numbers, relative to this standard curve. Virus quantification by plaque assay was performed on
111 BHK-21 monolayers in 6-well plates under an overlay of 1% methylcellulose (Morales et al., 2010).
112 Infected cells were cultured 7 days at 30°C in 5% CO₂. Overlay media was aspirated and cells were
113 stained for 10 min with 1% crystal violet in 20% ethanol.

114 2.5. XNC10 tetramer production

115 XNC10 tetramers were generated as previously described (Edholm et al., 2013). Briefly, beta 2
116 microglobulin (b2m) was linked via a 23-aa Glycine rich C-terminal flexible linker to the α 1- α 3
117 domains of XNC10 containing a BirA site-specific biotinylation site at the end of the α 3 domain and
118 cloned into the pMIBV5-HisA expression vector (Invitrogen). The b2m-linker-XNC10 construct was
119 expressed in Sf9 insect cells and monomeric b2m-linker-XNC10 was purified by Ni-NTA-Agarose
120 Chromatography (Qiagen) and concentrated to 1 µg/µL using Amicon Ultra Centrifugal Filter
121 (Millipore). BirA enzymatic biotinylation was performed for 18 h at 30 °C according to the
122 manufacturer's protocol (Avidity), and the purified biotinylated proteins were extensively dialyzed
123 against APBS, pH 7.5, to remove any unbound biotin. XNC10 tetramers were generated by incubating
124 b2m-linker-XNC10 with fluorochrome-labeled streptavidin at a 5:1 ratio at room temperature for 4
125 hours before use. Purified XNC10 tetramers (1 µg) were injected intra i.p. in a volume of 5 µl.

126 2.6. Statistical analysis

127 The Mann-Whitney U and ANOVA as well as non-parametric Kruskal-Wallis tests were used
128 for statistical analysis of expression and viral load data. Analyses were performed using a Vassar Stat
129 online resource (<http://vassarstats.net/utest.html>). Statistical analysis of survival data was
130 performed using a Log-Rank Test (GraphPad Prism 6). A probability value of $p < 0.05$ was used in
131 all analyses to indicate significance. Error bars on all graphs represent the standard error of the mean
132 (SEM).

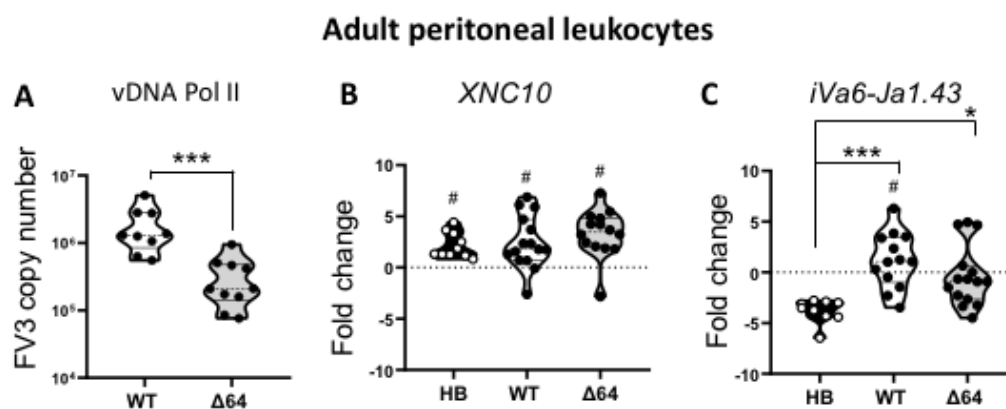
133 3. Results

134 3.1. Relationships between FV3 infection magnitude and iVa6 T cell response in adult *X. laevis*

135 We have previously demonstrated that FV3 infection in adult *X. laevis* elicit a transitory influx
136 of the innate (i)T cell subset iVa6 T into the peritoneal cavity (Edholm et al., 2015). To delineate the

137 factors governing iVα6 T cell recruitment during a FV3 infection, we took advantage of the FV3 KO
 138 mutant ΔvCARD (64R)-FV3 that has previously been shown to have attenuated virulence and growth
 139 *in vivo* elicit different host responses (Andino Fde et al., 2015; Jacques et al., 2017). Accordingly, we
 140 i.p infected adult *X. laevis* with wild type (WT) FV3 or Δ64-FV3 for 24 hours before collecting
 141 peritoneal leukocytes (PLs) and quantified transcript levels of the specific invariant Vα6-Jα1.43
 142 rearrangement. As a control we also challenged frogs with heat killed *E. coli*. This type of bacterial
 143 stimulation has been shown to induce a strong nonspecific inflammatory response but does not
 144 stimulate the recruitment or accumulation of iVα6 T cells in the peritoneal cavity (Edholm et al.,
 145 2015). Because iVα6 T cells interact with the MHC class I like molecule XNC10, we also examined its
 146 gene expression profile. To evaluate viral loads, we determined the FV3 genome copy number using
 147 absolute qPCR. Consistent with previous findings, Δ64-FV3 infection resulted in significantly ($P =$
 148 0.005) lower viral load compared to WT-FV3 already at 1 dpi (Jacques et al., 2017). All treatments
 149 resulted in a significant increased XNC10 expression compared to PLs collected from APBS injected
 150 control frogs at the same time point with no difference among the treatment groups (Fig. 1B).
 151 However, only WT-FV3 infection resulted in significantly elevated iVα6-Jα1.43 transcript levels
 152 compared to uninfected controls ($P = 0.018$), whereas in frogs injected with heat killed bacteria iVα6-
 153 Jα1.43 expression was lower compared to controls, presumably due to the large influx of immune
 154 cells into the peritoneal cavity. Although the high individual variation prevented statistical
 155 significance among the two FV3 infected groups, iVα6-Jα1.43 transcript levels observed with Δ64-
 156 FV3 mutants was elevated above sham-infect APBS controls in only 20% of frogs (3 out of 15 frogs)
 157 compared to 70% (9 out of 13) for WT-FV3 infected frogs, suggesting a correlation between iVα6
 158 recruitment and the level of viral replication.

Fig 1



159

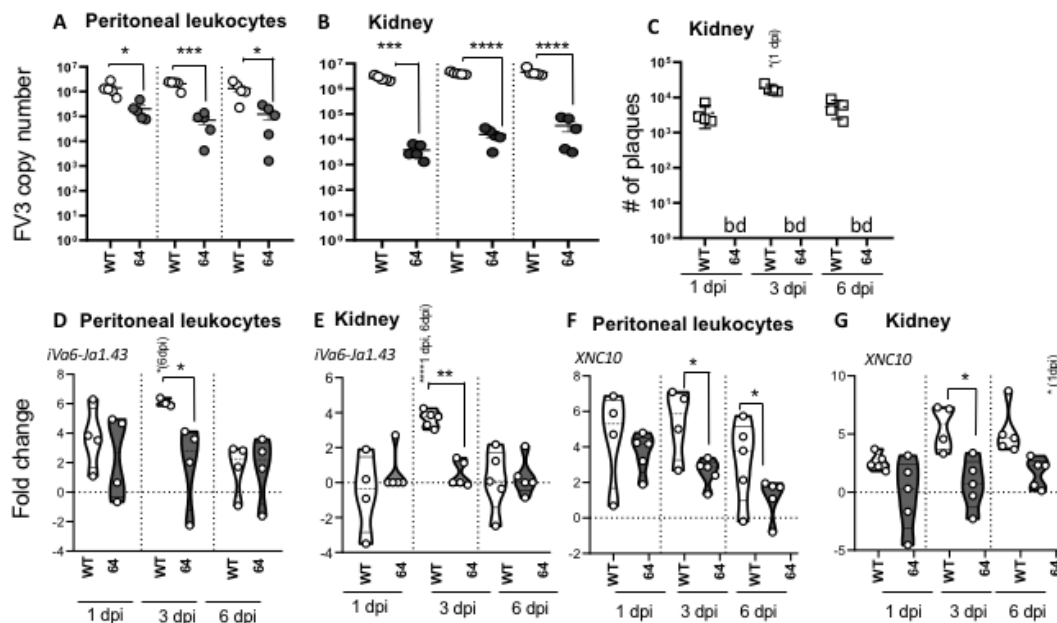
160 **Figure 1.** Effects of infection with attenuate KO FV3 recombinant or bacterial stimulation on iVα6 T
 161 cell response. PLs were collected at 1 dpi from adult frogs infected with 1×10^6 PFUs of WT- FV3 or
 162 Δ64-FV3, or 100 μl heat-killed (HB) *E. coli*. (A) Genome copy number using absolute qPCR with
 163 primers against FV3 polymerase II. (B) XNC10 relative gene expression and (C) iVα6-Jα1.43 relative
 164 gene expression. Gene expression was determined relative to an endogenous control (GAPDH) and
 165 fold changes were calculated using the unstimulated sample (injected with equivalent volume of
 166 APBS) collected at the same time point. Data are pooled from three independent experiments with
 167 $n = 4-5$ animals in each experiment and each dot represents an individual animal. The line intersecting
 168 the y -axis at 0 represents the unstimulated control that the fold changes of the treatments are in
 169 relation to. # denotes significant differences compared to unchallenged (APBS) injected controls and
 170 * $p < 0.05$ and *** $p < 0.001$ above the line denotes statistically significant differences between the
 171 indicated groups (one way ANOVA and Dunns's multiple comparisons test).

172 To obtain additional evidence of the correlation between active viral replication and iVα6 T cell
 173 recruitment, we i.p infected adult *X. laevis* with WT- and Δ64-FV3, and then monitored the transcript
 174 levels of iVα6-Jα1.43 and XNC10 in the peritoneal cavity (the site of infection) and kidney (main site
 175 for viral replication) at 1, 3 and 6 dpi (Fig. 2). To evaluate viral replication, we determined the genome
 176 copy number by absolute qPCR (Fig. 2A and 2B) and to assess productive infection we performed
 177 plaque assays (Fig. 2C and Fig. S1). Again Δ64-FV3 exhibited a severe replication defect preventing
 178 the production of infectious particles (Fig. 2C and Fig. S1). Using iVα6-Jα1.43 expression as a proxy
 179 for monitoring the kinetics of iVα6 T cell recruitment, we detected an increase in iVα6-Jα1.43
 180 transcript levels in the peritoneal cavity as early as 1 dpi with WT-FV3 compared to uninfected
 181 controls, which became significant by 3 dpi, and then returned to low but detectable levels by 6 dpi
 182 (Fig. 2D). In contrast, Δ64-FV3 infection did not trigger significant increase in iVα6-Jα1.43 transcript
 183 levels. In kidneys, iVα6-Jα1.43 expression was significantly elevated at 3 dpi and then returned to
 184 baseline at 6 dpi following infection with WT-FV3 (Fig. 2E). In contrast, no significant changes in
 185 iVα6-Jα1.43 expression was detected with Δ64-FV3 infection.

186 The examination of the expression response of the iVα6 T cell restricting MHC class I-like XNC10
 187 gene revealed some interesting correlations. In PLs, WT-FV3 infection induced a rapid (from 1 dpi)
 188 and sustained (until 6 dpi) XNC10 increase (Fig. 2F), which was delayed (from 3 to 6 dpi) in kidneys
 189 (Fig. 2G). Consistent with the poorly induced iVα6-Jα1.43 expression, infection with Δ64-FV3 also
 190 resulted in impaired induction of XNC10 gene expression. Indeed, Δ64-FV3 infection did not induce
 191 any significant change in XNC10 gene expression at 3 and 6 dpi in both PLs and kidneys.

192 Collectively, these data indicate that XNC10-restricted iVα6 T cell recruitment is relative to viral
 193 burden and requires active viral replication.

Fig 2



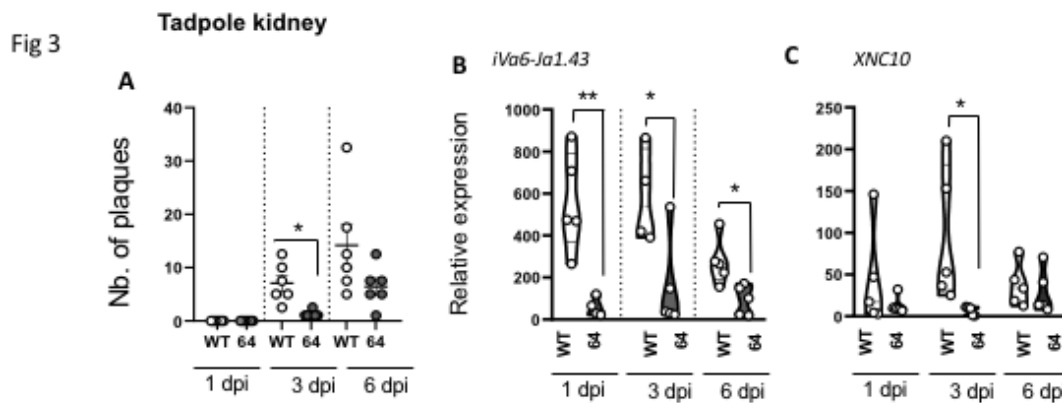
194

195 **Figure 2.** Magnitude of iVα6 T cell response in adult frogs is associated to the level of viral replication
 196 and production of infectious particles. PLs and kidneys were collected at 1, 3 and 6 dpi from adult
 197 frogs infected with 1×10^6 PFUs of WT-or Δ64-FV3. FV3 genome copy number by absolute qPCR in
 198 PLs (A) and kidneys (B) were determined and the total number of infectious particles in the kidney
 199 was determined by plaque assay (C). Gene expression of iVα6-Jα1.43 and XNC10 in PLs (D, F) and
 200 kidney (E, G) were determined relative to an endogenous control (GAPDH) and fold changes were
 201 calculated using mock-infected frogs as a control. Each dot represents an individual animal (n = 4-
 202 5). The line intersecting the y-axis at 0 represents the APBS control that the fold changes of the
 203 treatments are in relation to. * p<0,05; **p<0.01; ***p<0.001 and **** p<0.0001 above the line denotes
 204 statistically significant differences between the different treatment groups, significant differences

205 between timepoints within each treatment group is indicated in brackets (one way ANOVA and
206 Dunns's multiple comparisons test).

207 3.2. Relationships between FV3 infection magnitude and iVa6 T cell response in tadpoles

208 In contrast to adult frogs that exhibit a prominent conventional antiviral CD8 T cell response
209 restricted by classical MHC class Ia, tadpoles have barely detectable class Ia surface protein
210 expression and rely heavily on XNC10-restricted iVa6 T cells (Edholm et al., 2013). Indeed, XNC10-
211 deficient transgenic tadpoles lacking iVa6 T cells succumb to FV3 infection much faster than controls.
212 This suggests that a rapid iVa6 T cell response is required during the early stage of FV3 infection.
213 Similar to adult frogs, we postulated that the efficient recruitment of iVa6 T cells at the site of
214 infection would depend on a productive FV3 infection. Accordingly, we i.p. infected tadpoles with
215 either WT- or $\Delta 64$ -FV3. Consistent with previous reports, $\Delta 64$ -FV3 exhibited a severe growth defect
216 in tadpoles as shown by the very low number of plaques detected even at 6 dpi (Fig. 3A and Fig. S2).
217 As expected, WT FV3 infection elicited an iVa6 T cell response that was overall comparable to adults
218 including an early (by 1 dpi) increase in iVa6-Ja1.43 as well as XNC10 transcript levels that were
219 maintained by 3 dpi and then declined close to background levels by 6 dpi. In contrast, there were no
220 significant changes in XNC10 and iVa6-Ja1.43 transcript levels following $\Delta 64$ -FV3 infection (Fig. 3B).



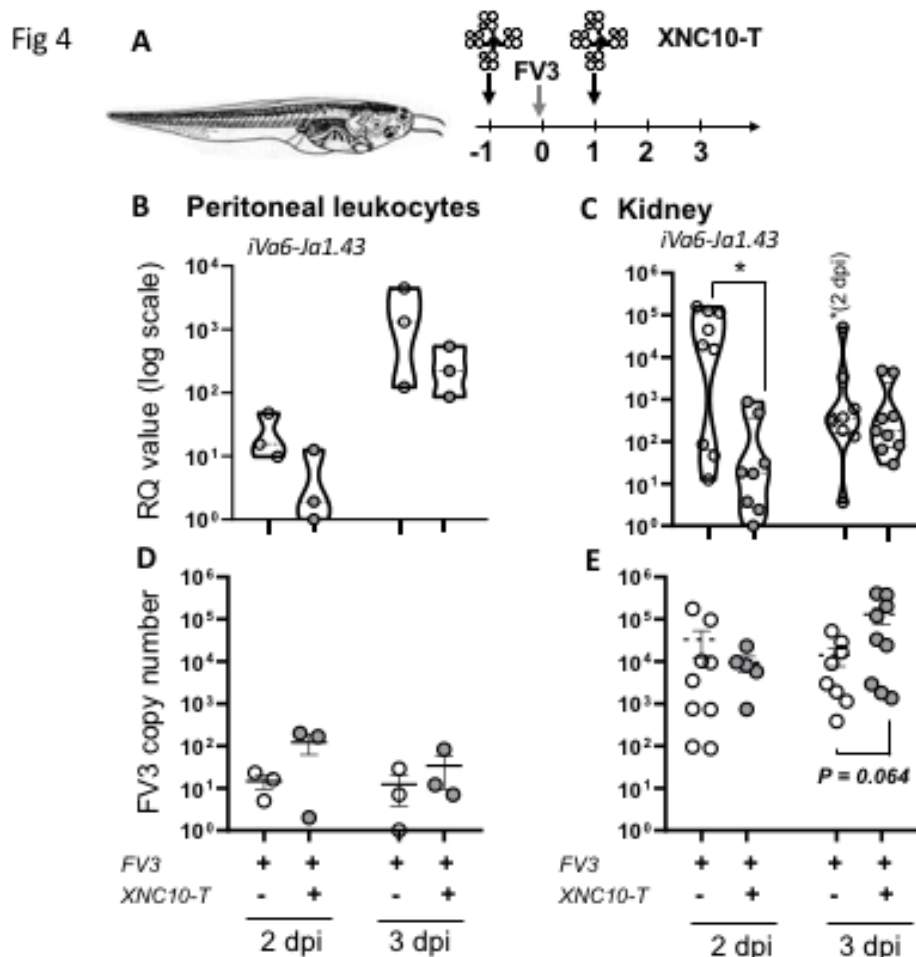
221

222 **Figure 3.** iVa6 T cell response in tadpoles depends on active viral replication and productive FV3
223 infection. Three week-old (stage 55) tadpoles were infected with 10,000 PFUs of WT-or $\Delta 64$ -FV3. At 1,
224 3 and 6 dpi kidneys were collected and the total number of infectious particles were determined by
225 plaque assay respectively (A). Gene expression of iVa6-Ja1.43 (B) and XNC10 (B) was determined
226 relative to an endogenous control (GAPDH) and relative expression was calculated against the lowest
227 observed expression according to the $\Delta\Delta Ct$ method (n =5). No iVa6-Ja1.43 transcripts were detected
228 in the kidney uninfected tadpoles. * $p < 0.05$ and ** $p < 0.01$ above the line denotes statistically significant
229 differences between treatment groups. (one way ANOVA and Dunn's multiple comparisons test).

230 3.3. Targeted iVa6T cell depletion in vivo

231 As mentioned, intraperitoneal (i.p) infection of *X. laevis* tadpoles with FV3 results in a rapid and
232 transitory increase in Va6-Ja1.43 transcript levels, both at the site of infection and in the kidney (main
233 FV3 target organ), consistent with a direct and active involvement of this specific iT cell population
234 in the early anti-FV3 response (Edholm et al., 2015). In support of this possibility, the developmental
235 disruption of iVa6 T cells in MHC class I-like XNC10- deficient transgenic tadpoles, results in
236 increased susceptibility to FV3 (Edholm et al., 2013). However, silencing of XNC10 from early
237 embryogenesis is likely to result in biological effects other than those inferred via the reciprocal loss
238 of a unique iT cell population. Therefore, to more directly determine the role of iVa6 T cells in anti-
239 viral defense against FV3 in the presence of a functional XNC10 gene, we targeted iVa6 T cells using
240 XNC10 tetramers. XNC10 tetramers have been shown to selectively induce iVa6T cell death *ex vivo*

241 and to temporarily ablate $V\alpha 6\text{-J}\alpha 1.43$ transcript levels *in vivo* (Banach et al., submitted). Accordingly,
 242 we injected *X. laevis* tadpoles with 1 μg of XNC10 tetramers 1 day prior and 1 day following i.p.
 243 injection with FV3 and quantified transcript levels of the invariant $V\alpha 6\text{-J}\alpha 1.43$ rearrangement in PLs
 244 and kidney at different times following infection (Fig. 4). Control groups received injections with an
 245 equivalent volume of amphibian PBS at the same time points. To evaluate viral loads and
 246 dissemination in the different groups we determined the FV3 genome copy number using absolute
 247 qPCR (Fig. 4D-E). In addition, we examined the gene expression of XNC10 to evaluate any impact of
 248 the injection regime on the expression of this MHC class I-like gene (Fig. S3).



249

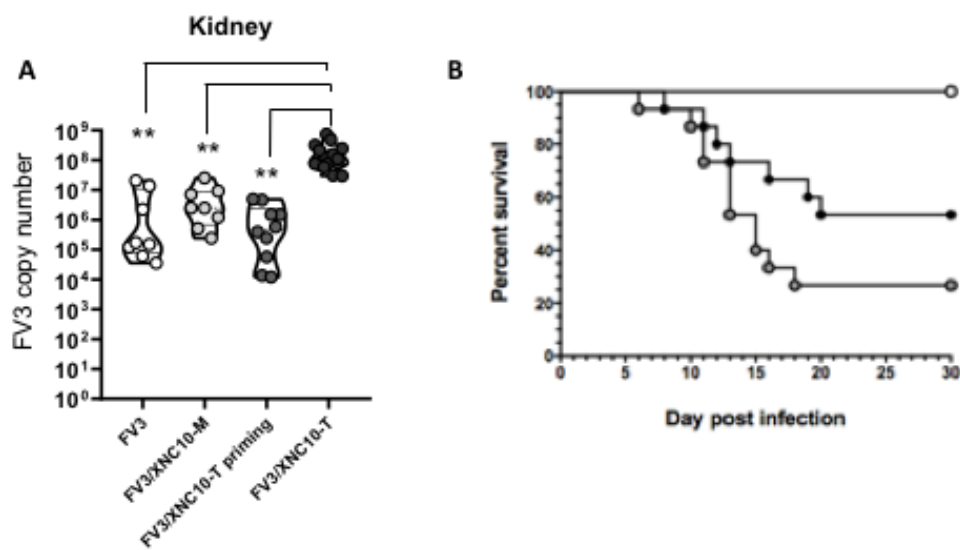
250 **Figure 4.** XNC10 tetramer-mediated iVa6T cell depletion in tadpoles affects iVa6-Ja1.43 transcript
 251 levels and viral replication. PLs and kidneys were collected from three weeks-old (stage 55) tadpoles
 252 that had been injected with 1 μg XNC10 tetramers or vehicle control 1 day pre and 1 day post i.p.
 253 injected with 10,000 PFUs of FV3, at the indicated time points (n = 9). A schematic of the injection
 254 regime is shown in A. Gene expression of iVa6-Ja1.43 in PLs (B) and kidney (C) is shown. Results are
 255 normalized to an endogenous control and presented as relative expression compared with the lowest
 256 observed value according to the $\Delta\Delta\text{Ct}$ method. FV3 loads in PLs (D) and kidney (E) were measured
 257 using absolute qPCR with primers against FV3 polymerase II. For peritoneal leukocytes each dot
 258 represents a pool of 3 tadpole while for kidney each dot represents a single tadpole. * $p < 0.05$ denotes
 259 statistically significant differences between the indicated groups (One way ANOVA followed by
 260 Tukey's multiple comparisons test).

261 Consistent with XNC10 tetramers inducing iVa6 T cell death, iVa6-Ja1.43 transcripts were
 262 markedly reduced, albeit not significantly, in the peritoneal cavity (site of infection) at 2 dpi, and
 263 remained lower than controls at 3 dpi. In the kidney, iVa6-Ja1.43 transcripts were significantly lower
 264 in the XNC10 tetramer treated group at 2 dpi, reaching levels equivalent to controls by 3 dpi. It is

265 noteworthy that consistent with previous reports, *iVα6-Jα1.43* transcripts were either undetected or
 266 near threshold levels in uninfected tadpoles. Thus, XNC10 tetramer treatment provides an efficient
 267 transient depletion of *iVα6* T cells *in vivo* providing us with a system to directly investigate the
 268 functional roles of *iVα6* T cells. No significant difference was observed in XNC10 expression between
 269 the two groups (Fig. S3).

270 In regards to viral loads, while there was no significant difference in viral genome copy numbers
 271 in the peritoneal cavity, XNC10 tetramer treated tadpoles displayed a marginally significant (P
 272 $=0.064$) higher viral load in the kidney by 3 dpi. By 6 dpi, using the same injection scheme as described
 273 in Fig. 4A, there were significantly higher viral loads in the kidney of the XNC10-tetramer treated
 274 group compared to vehicle control (Fig. 5). Notably, viral loads were not increased in tadpoles
 275 injected with XNC10 monomers, which do not bind to *iVα6* T cells (Edholm et al., 2013). In addition,
 276 XNC10 tetramer treatment had only a transitory effect on *iVα6* T antiviral activity as shown by
 277 comparable viral loads detected when FV3 infection occurred 3 days rather than 1 day after XNC10
 278 tetramer injection (Fig 5A). To assess whether this increase in viral loads had an impact on host
 279 resistance, we determined the cumulative mortality and mean survival of XNC10 tetramer injected
 280 and FV3 challenged tadpoles (Fig 6). Notably, transitory depletion of antiviral *iVα6* T cells within 24
 281 hours of FV3 infection resulted in increased mortality rate compared with FV3 infected controls (P
 282 $=0.0568$). These data support the conclusion that *iVα6* T cells are intricately involved in *X. laevis* anti-
 283 FV3 immune responses and highlights the importance of an efficient onset of appropriate anti-viral
 284 immune response in order to control and efficiently combat FV3 infection.

Fig 5



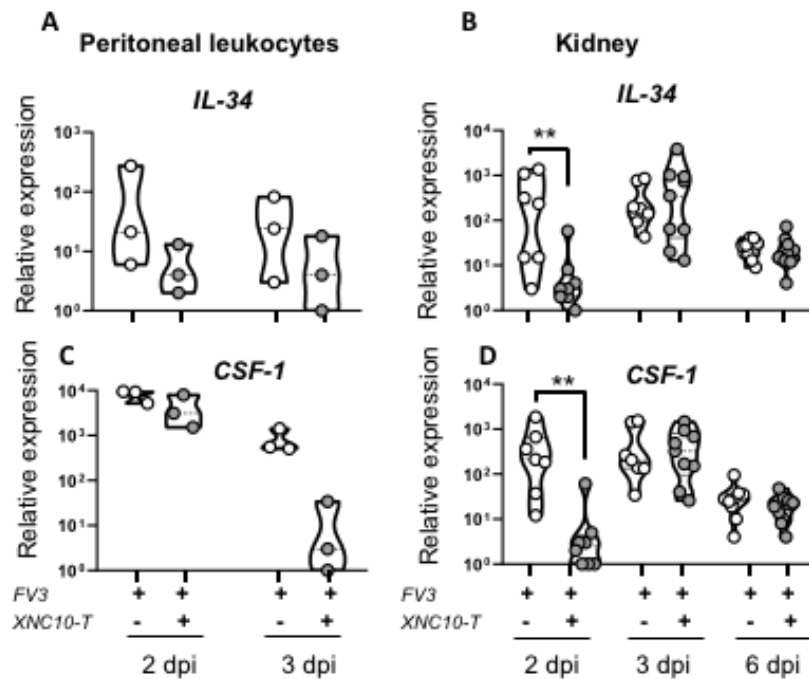
285

286 **Figure 5. Specificity and long term impact of transitory *iVα6*T cell depletion.** (A) Three week-old
 287 (stage 55) tadpoles were injected with either 1 μ g XNC10- tetramers, 1 μ g XNC10- monomers or
 288 vehicle control 1 day pre and 1 day post i.p injected with 10,000 PFUs of FV3 ($n=8$) and kidneys were
 289 collected at 6 dpi. Viral loads were assessed by absolute qPCR with primers against FV3 polymerase
 290 II. The results are combined from two separate experiments and each dot represents an individual
 291 tadpole. ** $p < 0.01$ and *** $p > 0.0005$ above the line denotes statistically significant differences between
 292 the indicated groups (One way ANOVA followed by Tukey's multiple comparisons test). (B) Three
 293 week-old (stage 55) tadpoles were injected with either 2 μ g XNC10 tetramers or vehicle control 1 day
 294 pre and 1 day post i.p injected with 10,000 PFUs of FV3 ($n=X$) and survival was monitored daily over
 295 a 30-day period. Survival was determined using Kaplan-Meier, * $p < 0.05$, ** $p > 0.005$ and *** $p > 0.0005$.
 296 Uninfected controls (white circle), FV3 infected tadpoles (black circle) and XNC10 tetramer treated
 297 FV3 infected tadpoles (grey circle).

298 3.4. Effects of *iVa6T* cell depletion on PLs and kidney antiviral responses in tadpoles.

299 We have previously shown that the compromised anti-FV3 response observed in XNC10-
 300 deficient transgenic frogs correlates with the induction of macrophages exhibiting a less potent
 301 antiviral state (Edholm et al., 2013). In particular, XNC10 deficiency hampered the expression of the
 302 macrophage growth factor IL-34. Notably IL-34 has been shown to elicit the differentiation of
 303 mononuclear phagocytes into robust type I interferon producing macrophages exhibiting strong FV3
 304 antiviral activity (Grayfer and Robert, 2014). These findings prompted us to hypothesize that *iVa6* T
 305 cells promote timely and efficient type I interferon (IFN)-mediated anti-FV3 responses by influencing
 306 the polarization of macrophages into a more potent antiviral state. Thus, to further delineate the
 307 putative functional roles of *iVa6* T cells during FV3 infection we next determined if direct and
 308 transient *iVa6* T cell depletion has an impact on macrophage effector functions. To address this
 309 possibility, we monitored the expression profiles of the two macrophage growth factors CSF-1
 310 (Grayfer and Robert, 2013) and IL-34 (Grayfer and Robert, 2014) in peritoneal leucocytes and kidney
 311 (Fig. 6) from FV3 infected tadpoles with or without XNC10 tetramer treatment. Both IL-34 and CSF-
 312 1 transcription levels were significantly lower in the kidney of XNC10 tetramer treated tadpoles at 2
 313 dpi, correlating with the reduced *iVa6-Jα1.43* expression and reached levels comparable to controls,
 314 by 3 dpi.

Fig 6

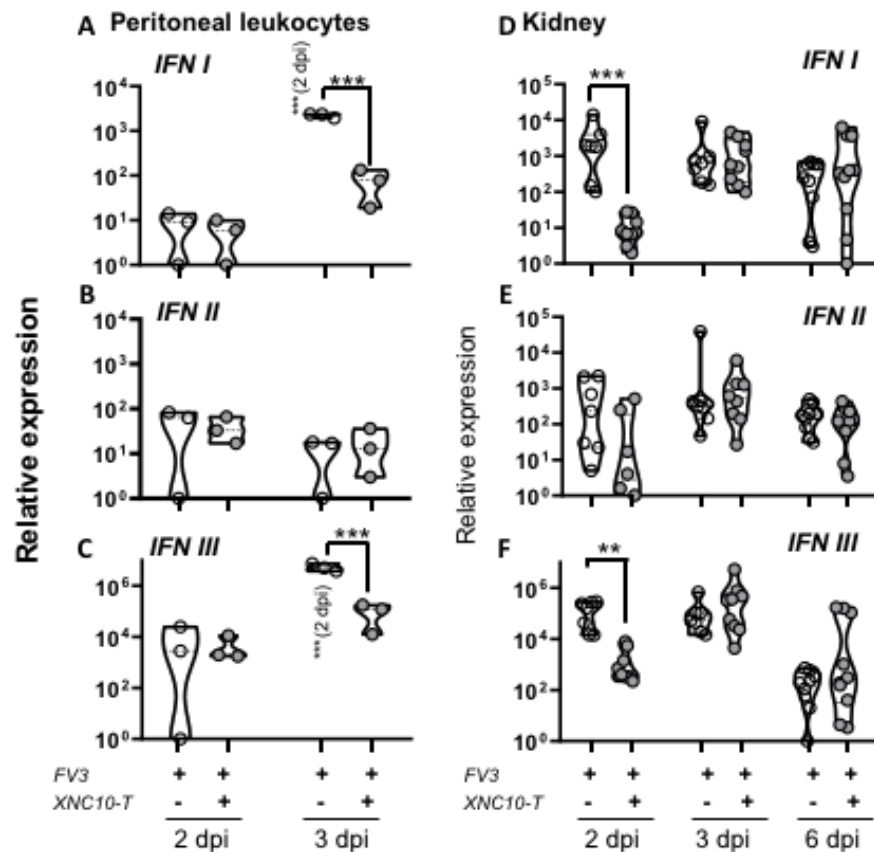


315

316 **Figure 6.** Effect of XNC10 tetramer treatment on the expression of the macrophage stimulating factor
 317 genes CSF1 and IL-34 in peritoneal cavity and kidney of FV3 infected tadpoles. PLs and kidneys were
 318 collected from three weeks-old (stage 55) tadpoles that had been injected with 1 μ g XNC10 tetramers
 319 or vehicle control 1 day pre- and 1 day post-ip injected with 10,000 PFUs of FV3, at the indicated time
 320 points (n=8-9). Quantitative gene expression analysis of IL-34 (A, B) and CSF-1 (C, D) were determined
 321 relative to an endogenous control (GAPDH) and relative expression was calculated against the lowest
 322 observed expression according to the $\Delta\Delta$ Ct method (n=9), * p<0,05, ** p<0.005 and ***p>0.001 above
 323 the line denotes statistically significant differences between the different treatment groups, significant
 324 differences between timepoints within each treatment group is indicated in brackets (One way
 325 ANOVA followed by Tukey's multiple comparisons test).

326 Given that the type I IFN response is critical in controlling viral infections and is compromised
 327 in XNC10-deficient animals (Edholm et al., 2015), we postulated that a direct impairment of $iV\alpha 6$ T
 328 cells should affect type I IFN gene expression to a similar extent. Indeed, unlike control animals, both
 329 type I IFN and type III IFN gene expression were magnitudes lower at 3 dpi in PLs of XNC10 tetramer
 330 treated animals compared to controls, whereas the levels of type II IFN was highly variable between
 331 animals with no apparent difference in expression between the two groups (Fig 7A-C). Similarly, in
 332 kidneys the expression of both type I and type III IFN genes was significantly impaired in XNC10
 333 tetramer treated animals at 2 dpi, whereas by 3 dpi both treated and control groups exhibited high
 334 transcript levels of type I and type III IFN (Fig. 7D-E).

Fig 7



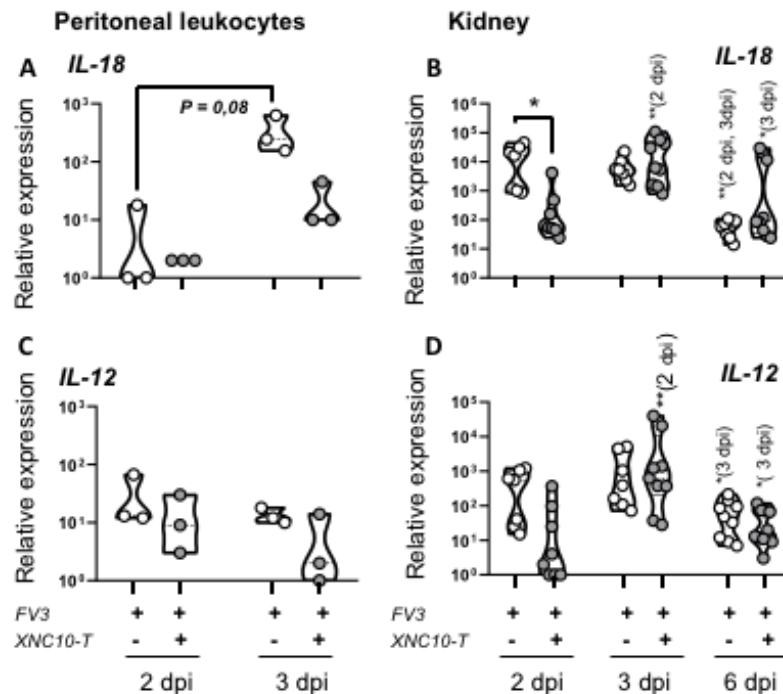
335

336 **Figure 7.** XNC10 tetramer treatment results in a delayed antiviral response in peritoneal cavity and
 337 kidney of FV3 infected tadpoles. PLs and kidneys were collected from three weeks-old (stage 55)
 338 tadpoles that had been injected with 1 μ g XNC10 tetramers or vehicle control 1 day pre- and 1 day
 339 post-ip injected with 10,000 PFUs of FV3, at the indicated time points (n= 8-9). Quantitative gene
 340 expression analysis of type I (A, D), type II (B, E) and type III IFN (C, F) were determined relative to
 341 a endogenous control (GAPDH) and relative expression was calculated against the lowest observed
 342 expression according to the $\Delta\Delta$ Ct method (n =9), * p< 0,05, ** p<0,005 and ***p>0,001 above the line
 343 denotes statistically significant differences between the different treatment groups, significant
 344 differences between timepoints within each treatment group is indicated in brackets (One way
 345 ANOVA followed by Tukey's multiple comparisons test).

346 In response to a viral infection, protective host response relies on the onset of appropriate cell
 347 mediated immunity to mediate viral clearance. Thus, we next examined the expression of
 348 interleukin18 (IL-18) and interleukin 12 (IL-12) upon FV3 infection in PLs and kidney of control and
 349 $iV\alpha 6$ T cell deficient tadpoles. Both IL-18 and IL-12 are produced by macrophages and act in synergy
 350 to promote the development of innate and specific Th1 type immune responses (Barbarin et al., 2017;
 351 Huber et al., 2015; Zajonc and Girardi, 2015). Given that $iV\alpha 6$ T cell deficiency hampers the induction
 352 of macrophage differentiating factors resulting in a delayed interferon response, we postulated that
 353 IL-18 and IL-12 cytokine production would be similarly impaired. Indeed, unlike control animals, IL-

354 18 expression was significantly lower at 2 dpi in kidney of XNC10 tetramer treated animals, whereas
 355 at 3 dpi XNC10 tetramer treated tadpoles exhibited elevated IL-18 transcript levels on par with that
 356 of controls that were significantly reduced by 6 dpi in both groups (Fig. 8). While there was a slight
 357 decrease in IL-12 gene expression at 2 dpi in XNC10 tetramer treated animals, it was not statistically
 358 significant.

Fig 8



359

360 **Figure 8.** Effects of iVa6T cell depletion on IL-18 and IL-12 responses. PLs and kidneys were collected
 361 from three weeks-old (stage 55) tadpoles that had been injected with 1 μ g XNC10 tetramers or vehicle
 362 control 1 day pre and 1 day post i.p injected with 10,000 PFUs of FV3, at the indicated time points (n=
 363 8-9). Quantitative gene expression of IL-18 (A-B) and type IL-12 (C-D) was determined relative to an
 364 endogenous control (GAPDH) and relative expression was calculated against the lowest observed
 365 expression according to the $\Delta\Delta$ Ct method (n =9), * p<0.05; ** p<0.005 and ***p>0.001 above the line
 366 denotes statistically significant differences between the different treatment groups, significant
 367 differences between timepoints within each treatment group is indicated in brackets (One way
 368 ANOVA followed by Tukey's multiple comparisons test).

369 Overall, these findings are in accordance with what was previously been reported for XNC10-
 370 deficient transgenic animals (that lack both XNC10 and iVa6 T cells, (Edholm et al., 2015)) suggesting
 371 that iVa6 T cells are directly and critically involved in mounting an anti-FV3 response, and that acute
 372 loss or impairment of these cells result in both a delayed type I and type III IFN antiviral response as
 373 well as a delayed IL-18 response.

374 4. Discussion

375 The present study provides new insights into the requirement for an effective amphibian host
 376 response to the ranavirus FV3 through an early detection by the MHC class I-like XNC10 and the rapid
 377 recruitment of the activated XNC10-restricted innate T cell subset iVa6. A remarkable feature of this
 378 novel antiviral immune surveillance system is that it is prominent in naturally classical MHC class
 379 Ia-deficient tadpoles, whereas it is a component in class Ia and conventional T cell competent adults.
 380 Nevertheless, while this antiviral system is central for tadpole survival at early stage of FV3 infection,
 381 it is also critical for a timely control of viral burden in adult frogs. To better functionally define this
 382 novel antiviral immune surveillance system, we examined the initial conditions of FV3 infection that
 383 trigger the iVa6 T cell response by using a deficient FV3 recombinants and we defined the antiviral
 384 immune response initiated by iVa6 T cells.

385 The critical role of iNKT cells in antiviral immunity is well documented in mammals, where
386 their pre-activated or memory phenotypes allow them to serve as early responder (within hours
387 following infection) without requiring expansion as conventional T cells (Juno et al., 2012; Kohlgruber
388 et al., 2016). Similarly, in *X. laevis* we have shown a rapid increase of iV α 6-J α 1.43 transcript levels
389 (within 1 dpi) at the site of FV3 infection in the peritoneum and in the main site of viral replication in
390 the kidney, concomitant with a decrease in the spleen. Notably, the recruitment of these iV α 6 cells
391 occurs days before significant proliferation of conventional T cells, which become significant only
392 from 3 dpi onward in the spleen (Morales and Robert, 2007). This strongly suggests that iV α 6 T cell
393 are rapidly activated and recruited from the spleen by FV3 infection (Edholm et al., 2015).

394 Here, we provide further evidence that iV α 6 T cell recruitment occurs in direct response to FV3
395 infection and is not indirectly triggered by inflammation induced by heat-killed bacteria or by a
396 replication-defective Δ 64-FV3 recombinant. Furthermore, while both attenuated Δ 64-FV3 and heat-
397 killed bacterial stimulation induced an early transcriptional induction of the MHC class I-like XNC10
398 that restricts iV α 6 T cells, these elevated expression levels were only maintained in WT-FV3 infected
399 frogs. This suggests a coordinated role of XNC10 and iV α 6 T cells in detecting and eliciting a rapid
400 response against ranavirus pathogens. This coordinate response of XNC10 and iV α 6 T cells only
401 induced by a productive viral infection is also consistent with the detection of virally-derived
402 products or ligands. Whether XNC10 bind ligand(s) and if so the identity of such putative XNC10
403 ligand(s) is currently unknown, but nucleotide sequence comparisons and 3D-modelling of the
404 putative ligand binding regions indicate that XNC10 could accommodate lipid ligands in a way
405 reminiscent to CD1d (Edholm et al., 2014; Goyos et al., 2011; Rossjohn et al., 2012). Thus, it is tempting
406 to speculate that XNC10 can be upregulated and bind products/ligands from early FV3 replication
407 and/or release of assembled viruses to activate iV α 6 T cell response. In this scenario, infection by Δ 64-
408 FV3 would not lead to sufficient production and release of FV3-derived products/ligands to initiate
409 iV α 6 T cell recruitment and activation.

410 Interestingly, the correlation between defective viral replication, blunted XNC10 gene
411 expression response and impaired iV α 6 T cell recruitment was more robust in tadpoles. This may be
412 due to the heavier reliance on iT cells in tadpoles. In absence of an efficient classical MHC-I restricted
413 conventional CD8 T cell response, iV α 6 T cells are likely to be more directly and critically involved
414 in tadpole host response against FV3. This is evidenced by marked vulnerability of XNC10-deficient
415 transgenic tadpoles lacking iV α 6 T cell to FV3 infection, especially at early stages on infection
416 (Edholm et al., 2013). Our findings using XNC10 tetramer treatment substantiate this initial
417 requirement of iV α 6 T cell response for controlling viral infection and host resistance to FV3. Indeed,
418 a partial and transient depletion of iV α 6 T cells prompted by injection of XNC10 tetramers shortly
419 before and after infection impairs tadpole immune defenses, which not only leads to more severe
420 viral burden but also decrease survival rate.

421 While the effector functions of iV α 6 T cells are likely to be multifaceted, our previous findings
422 support a role of these cells as immune modulators influence the polarization of peritoneal
423 macrophages into a more robust anti-viral state (Edholm et al., 2015). It is noteworthy that the
424 expression of type I and III IFN as well as cytokine such as CSF-1 and IL-18 are transiently altered in
425 parallel to iV α 6 T cells depletion. Little is known about the iV α 6 T cell mechanism of action, but
426 previous findings have hinted at a modulation of macrophages (Edholm et al., 2013; Edholm et al.,
427 2015). While type I and III IFN is likely produced and released by many cell types, the rapid increase
428 of their transcript levels in the peritoneum and kidneys upon FV3 infection coincide with the
429 recruitment of monocytic phagocytes both in tadpoles and adult frogs (De Jesús Andino et al., 2012;
430 Grayfer et al., 2015; Morales et al., 2010). Infiltration of MHC class II+ leukocytes in kidneys at early
431 stage of FV3 infection is also consistent with infiltration of macrophages (Morales and Robert, 2007).
432 CSF1 and IL-34 are two key macrophage growth factors acting through the same CSF-1 receptor
433 across jawed vertebrates (Droin and Solary, 2010). In *X. laevis*, CSF1 is required for the commitment
434 and maturation of mature macrophage lineage cells (Grayfer and Robert, 2013), whereas IL-34
435 stimulates stronger antiviral effector function by macrophages both in tadpoles and adult frogs
436 (Grayfer and Robert, 2014, 2015). The acute decrease in type I and III IFN as well as CSF1 and IL-34

437 at 2 dpi concomitantly with the XNC10 tetramer-mediated iV α 6 T cell defect reinforce the postulated
438 functional link between iV α 6 T cell and macrophages. This, of course does not preclude possible
439 interaction of iV α 6 T cells with other immune cell effectors as well as a reciprocal effect of
440 macrophages on iV α 6 T cells. Indeed, macrophages in mammals are known to be important producer
441 of IL-12 and IL-18, two cytokines that stimulate iNKT cells and promote Th1 adaptive immune
442 response (Barbarin et al., 2017; Huber et al., 2015; Yasuda et al., 2019). The transitory blunted
443 expression of IL-18 and to a lesser extent IL-12 that accompanied iV α 6 T cell transient defect, besides
444 being consistent with decreased macrophage function may have amplified XNC10 tetramer-
445 mediated iV α 6 T cell impairment. In any case, it is remarkable that the brief interference of iV α 6 T
446 cell function has a long-lasting negative impact on the tadpole ability to control FV3 infection and
447 ultimately to survive infection.

448 **Acknowledgements:** We thank Tina Martin for animal husbandry. This work was supported by the National
449 Institute of Allergy and Infectious Diseases at the National Institutes of Health (grant number: R24-AI-059830),
450 the National Science Foundation (grant number: IOS- 1,456,213 and 1754274) and the Tromsø Research
451 Foundation Starting Grant.

452 References

- 453 Abboud, G., Tahiliani, V., Desai, P., Varkoly, K., Driver, J., Hutchinson, T.E., Salek-Ardakani, S., 2016. Natural
454 Killer Cells and Innate Interferon Gamma Participate in the Host Defense against Respiratory Vaccinia
455 Virus Infection. *J Virol* 90, 129-141.
- 456 Adams, E.J., Luoma, A.M., 2013. The adaptable major histocompatibility complex (MHC) fold: structure and
457 function of nonclassical and MHC class I-like molecules. *Annu Rev Immunol* 31, 529-561.
- 458 Andino Fde, J., Grayfer, L., Chen, G., Gregory Chinchar, V., Edholm, E.S., Robert, J., 2015. Characterization of
459 Frog Virus 3 knockout mutants lacking putative virulence genes. *Virology* 485, 162-170.
- 460 Barbarin, A., Cayssials, E., Jacomet, F., Nunez, N.G., Basbous, S., Lefevre, L., Abdallah, M., Piccirilli, N., Morin,
461 B., Lavoue, V., Catros, V., Piaggio, E., Herbelin, A., Gombert, J.M., 2017. Phenotype of NK-Like CD8(+) T
462 Cells with Innate Features in Humans and Their Relevance in Cancer Diseases. *Frontiers in immunology*
463 8, 316.
- 464 Borg, N.A., Wun, K.S., Kjer-Nielsen, L., Wilce, M.C., Pellicci, D.G., Koh, R., Besra, G.S., Bharadwaj, M., Godfrey,
465 D.I., McCluskey, J., Rossjohn, J., 2007. CD1d-lipid-antigen recognition by the semi-invariant NKT T-cell
466 receptor. *Nature* 448, 44-49.
- 467 Chen, G., Ward, B.M., Yu, K.H., Chinchar, V.G., Robert, J., 2011. Improved knockout methodology reveals that
468 frog virus 3 mutants lacking either the 18K immediate-early gene or the truncated vIF-2 α gene are
469 defective for replication and growth in vivo. *J Virol* 85, 11131-11138.
- 470 De Jesús Andino, F., Chen, G., Li, Z., Grayfer, L., Robert, J., 2012. Susceptibility of *Xenopus laevis* tadpoles to
471 infection by the ranavirus Frog-Virus 3 correlates with a reduced and delayed innate immune response in
472 comparison with adult frogs. *Virology*, In press.
- 473 Diana, J., Griseri, T., Lagaye, S., Beaudoin, L., Autrusseau, E., Gautron, A.-S., Tomkiewicz, C., Herbelin, A.,
474 Barouki, R., von Herrath, M., Dalod, M., Lehuen, A., 2009. NKT Cell-Plasmacytoid Dendritic Cell
475 Cooperation via OX40 Controls Viral Infection in a Tissue-Specific Manner. *Immunity* 30, 289-299.
- 476 Droin, N., Solary, E., 2010. Editorial: CSF1R, CSF-1, and IL-34, a "menage a trois" conserved across vertebrates. *J*
477 *Leukoc Biol* 87, 745-747.
- 478 Edholm, E.S., Albertorio Saez, L.M., Gill, A.L., Gill, S.R., Grayfer, L., Haynes, N., Myers, J.R., Robert, J., 2013.
479 Nonclassical MHC class I-dependent invariant T cells are evolutionarily conserved and prominent from
480 early development in amphibians. *Proc Natl Acad Sci U S A* 110, 14342-14347.
- 481 Edholm, E.S., Banach, M., Robert, J., 2016. Evolution of innate-like T cells and their selection by MHC class I-like
482 molecules. *Immunogenetics* 68, 525-536.
- 483 Edholm, E.S., Goyos, A., Taran, J., De Jesus Andino, F., Ohta, Y., Robert, J., 2014. Unusual evolutionary
484 conservation and further species-specific adaptations of a large family of nonclassical MHC class Ib genes
485 across different degrees of genome ploidy in the amphibian subfamily Xenopodinae. *Immunogenetics* 66,
486 411-426.

- 487 Edholm, E.S., Grayfer, L., De Jesus Andino, F., Robert, J., 2015. Nonclassical MHC-Restricted Invariant Valpha6
488 T Cells Are Critical for Efficient Early Innate Antiviral Immunity in the Amphibian *Xenopus laevis*. *J*
489 *Immunol* 195, 576-586.
- 490 Goyos, A., Sowa, J., Ohta, Y., Robert, J., 2011. Remarkable conservation of distinct nonclassical MHC class I
491 lineages in divergent amphibian species. *J Immunol* 186, 372-381.
- 492 Gray, M.J., Chinchar, V.G., 2015. *Ranaviruses*. Springer Open, Heidelberg, New York, Dordrecht, London.
- 493 Grayfer, L., De Jesus Andino, F., Robert, J., 2015. Prominent amphibian (*Xenopus laevis*) tadpole type III
494 interferon response to the frog virus 3 ranavirus. *J Virol* 89, 5072-5082.
- 495 Grayfer, L., Robert, J., 2013. Colony-Stimulating Factor-1-Responsive Macrophage Precursors Reside in the
496 Amphibian (*Xenopus laevis*) Bone Marrow Rather than the Hematopoietic Sub-Capsular Liver. *J. Innate*
497 *Immun.*, 531-542.
- 498 Grayfer, L., Robert, J., 2014. Divergent antiviral roles of amphibian (*Xenopus laevis*) macrophages elicited by
499 colony-stimulating factor-1 and interleukin-34. *J Leukoc Biol* 96, 1143-1153.
- 500 Grayfer, L., Robert, J., 2015. Distinct functional roles of amphibian (*Xenopus laevis*) colony-stimulating factor-1-
501 and interleukin-34-derived macrophages. *J Leukoc Biol* 98, 641-649.
- 502 Huber, C.M., Doisne, J.M., Colucci, F., 2015. IL-12/15/18-preactivated NK cells suppress GvHD in a mouse model
503 of mismatched hematopoietic cell transplantation. *European journal of immunology* 45, 1727-1735.
- 504 Jacques, R., Edholm, E.S., Jazz, S., Odalys, T.L., Francisco, J.A., 2017. *Xenopus-FV3* host-pathogen interactions
505 and immune evasion. *Virology*.
- 506 Juno, J.A., Keynan, Y., Fowke, K.R., 2012. Invariant NKT cells: regulation and function during viral infection.
507 *PLoS Pathog* 8, e1002838.
- 508 Kohlgruber, A.C., Donado, C.A., LaMarche, N.M., Brenner, M.B., Brennan, P.J., 2016. Activation strategies for
509 invariant natural killer T cells. *Immunogenetics* 68, 649-663.
- 510 Morales, H.D., Abramowitz, L., Gertz, J., Sowa, J., Vogel, A., Robert, J., 2010. Innate immune responses and
511 permissiveness to ranavirus infection of peritoneal leukocytes in the frog *Xenopus laevis*. *J Virol* 84, 4912-
512 4922.
- 513 Morales, H.D., Robert, J., 2007. Characterization of primary and memory CD8 T-cell responses against ranavirus
514 (FV3) in *Xenopus laevis*. *J Virol* 81, 2240-2248.
- 515 Price, S.J., Garner, T.W., Nichols, R.A., Balloux, F., Ayres, C., Mora-Cabello de Alba, A., Bosch, J., 2014. Collapse
516 of amphibian communities due to an introduced Ranavirus. *Current biology : CB* 24, 2586-2591.
- 517 Raftery, M.J., Winau, F., Giese, T., Kaufmann, S.H., Schaible, U.E., Schonrich, G., 2008. Viral danger signals
518 control CD1d de novo synthesis and NKT cell activation. *European journal of immunology* 38, 668-679.
- 519 Rossjohn, J., Pellicci, D.G., Patel, O., Gapin, L., Godfrey, D.I., 2012. Recognition of CD1d-restricted antigens by
520 natural killer T cells. *Nat Rev Immunol* 12, 845-857.
- 521 Wesley, J.D., Tessmer, M.S., Chaukos, D., Brossay, L., 2008. NK Cell-Like Behavior of V α 14i NK T Cells during
522 MCMV Infection. *PLOS Pathogens* 4, e1000106.
- 523 Yasuda, K., Nakanishi, K., Tsutsui, H., 2019. Interleukin-18 in Health and Disease. *International journal of*
524 *molecular sciences* 20.
- 525 Zajonc, D.M., Girardi, E., 2015. Recognition of Microbial Glycolipids by Natural Killer T Cells. *Frontiers in*
526 *immunology* 6, 400.
- 527



© 2019 by the authors. Submitted for possible open access publication under the terms and conditions of the Creative Commons Attribution (CC BY) license (<http://creativecommons.org/licenses/by/4.0/>).